Fatty Acid-Binding Proteins Inhibit Hydration of Epoxyeicosatrienoic Acids by Soluble Epoxide Hydrolase†

Richard L. Widstrom,*,‡ Andrew W. Norris,§ Jon Van Der Veer,‡ and Arthur A. Spector‡

Department of Biochemistry, University of Iowa, College of Medicine, Iowa City, Iowa 52242, and Cellular and Molecular Physiology, Joslin Diabetes Center, One Joslin Place, Boston, Massachusetts 02215

Received June 6, 2003; Revised Manuscript Received August 13, 2003

ABSTRACT: Epoxyeicosatrienoic acids (EETs) are potent regulators of vascular homeostasis and are bound by cytosolic fatty acid-binding proteins (FABPs) with K_d values of ∼0.4 μM. To determine whether FABP binding modulates EET metabolism, we examined the effect of FABPs on the soluble epoxide hydrolase (sEH)-mediated conversion of EETs to dihydroxyeicosatrienoic acids (DHETs). Kinetic analysis of sEH conversion of racemic [^{3}H]11,12-EET yielded $K_m = 0.45 \pm 0.08$ μM and $V_{max} = 9.2 \pm 1.4$ μmol min^{-1} mg^{-1}. Rat heart FABP (H-FABP) and rat liver FABP were potent inhibitors of 11,12-EET and 14,15-EET conversion to DHET. The resultant inhibition curves were best described by a substrate depletion model, with $K_d = 0.17 \pm 0.01$ μM for H-FABP binding to 11,12-EET, suggesting that FABP acts by reducing EET availability to sEH. The EET depletion by FABP was antagonized by the co-addition of arachidonic acid, oleic acid, linoleic acid, or 20-hydroxyeicosatetraenoic acid, presumably due to competitive displacement of FABP-bound EET. Collectively, these findings imply that FABP might potentiate the actions of EETs by limiting their conversion to DHET. However, the effectiveness of this process may depend on metabolic conditions that regulate the levels of competing FABP ligands.

Epoxyeicosatrienoic acids (EETs)[1] are synthesized from arachidonic acid by cytochrome P450 epoxygenases and function primarily as autocrine and paracrine mediators in the cardiovascular system and kidney (*1*−*4*). EETs dilate blood vessels by activating smooth muscle large conductance Ca^{2+}-activated K^+ channels (*5*−*7*), enhance fibrinolysis through induction of a tissue plasminogen activator (*8*), reduce cytokine-induced endothelial adhesion molecule expression by inhibiting the activation of NF-κB (*9*), and stimulate mesangial cell proliferation by activating a tyrosine kinase-Src signal transduction pathway (*10*, *11*). The function of EETs also might be mediated indirectly by conversion to ω-hydroxy metabolites that activate PPARα (*12*) or conversion to chain-elongated or -shortened metabolites (*13*, *14*). In addition, EETs are incorporated into cell phospholipids and are released rapidly when cells are exposed to the Ca^{2+} ionophore (*15*−*18*), suggesting they may affect phospholipid-mediated signal transduction processes.

A major pathway of EET metabolism is hydration by soluble epoxide hydrolase (sEH) to the diol, dihydroxyeicosatrienoic acid (DHET) (*19*, *20*). Reduction of sEH activity has been shown to lower systemic blood pressure. For example, systemic administration of a sEH inhibitor reduces blood pressure in spontaneously hypertensive rats (*21*). Furthermore, disruption of the sEH gene in male mice lowers blood pressure (*22*). These findings indicate the importance of characterizing any potential modulators of EET conversion to DHET by sEH in vascular cells.

Fatty acid binding proteins (FABPs) constitute a family of low molecular weight, cytosolic proteins that avidly bind long chain fatty acids (*23*), facilitating fatty acid diffusion and modulating intracellular fatty acid metabolism (*24*). We previously found that heart FABP (H-FABP) and liver FABP (L-FABP) bind EETs with K_d values of ∼0.4 μM (*25*), leading to the hypothesis that FABPs may modulate EET metabolism. H-FABP is expressed in vascular endothelial cells (*26*), a major site of EET activity and metabolism. This suggests that H-FABP is a candidate modulator of sEH activity in the cardiovascular system. Herein, we investigate the effects of FABP on EET conversion by sEH and the mechanisms involved. These experiments focus on the 11,12-EET regioisomer because it is thought to be the endothelium dependent hyperpolarizing factor (EDHF) in the coronary circulation (*7*) and appears to have the most potent anti-inflammatory effect on the endothelium (*9*).

EXPERIMENTAL PROCEDURES

Fatty acid-free bovine serum albumin (BSA) was purchased from Intergen (Purchase, NY); silica gel G thin-layer chromatography plates were from Alltech Associates (Deerfield, IL); 11,12-EET, 14,15-EET, and other fatty acids were from Cayman (Ann Arbor, MI); and egg phosphatidylcholine was from Avanti Polar Lipids (Alabaster, AL).

† This work was supported by Grants HL49264, HL62984, and HL72845 from the National Heart, Lung, and Blood Institute (AAS) and T32-DK63702 from NIH (A.W.N.).

* Corresponding author. Tel: (319) 338-0581. Fax: (319) 339-7025. E-mail: richard-widstrom@uiowa.edu.

‡ University of Iowa.

§ Joslin Diabetes Center.

[1] Abbreviations: BSA, bovine serum albumin; DHET, dihydroxyeicosatrienoic acid; EET, epoxyeicosatrienoic acid; FABP, fatty acid-binding protein; 20-HETE, 20-hydroxyeicosatetraenoic acid; PGE_2, prostaglandin E_2; sEH, soluble epoxide hydrolase.

10.1021/bi034971d CCC: $25.00
Published on Web 09/19/2003

Preparation of ^{3}H-EETs and Sodium Salts of Fatty Acids. [5,6,8,9,11,12,14,15-^{3}H]Arachidonic acid (55 Ci/mmol, American Radiolabeled Chemicals, St. Louis, MO) was mixed with arachidonic acid to a final specific activity of 0.2 μCi/nmol. The solvent was evaporated under N_2, and the fatty acid was taken up in 2 mL of methylene chloride, followed by dropwise addition of 0.5 equiv of 3-chloroperoxybenzoic acid (dissolved in methylene chloride) over 1 min and incubation at 35 °C for 30 min with vigorous stirring. The reaction was quenched with 2 mL of ice-cold 30 mM $NaHCO_3$ (pH 7.8) and mixed for 2 min. The aqueous phase was removed, and the organic phase was washed twice with $NaHCO_3$ and three times with water. After the organic phase was dried, the residue was resuspended in acetonitrile/methanol/water (54:8:38) and separated by reverse-phase HPLC on a C18 Discovery column (5 μm, 4.6 × 250 mm, Supelco, St. Louis, MO). The column was equilibrated in 15% solvent B ($CH_3CN/CH_3OH/H_2O$/HCOOH, pH 4.0, 540:80:380:0.0003 v/v) in solvent A (acetonitrile) at a flow rate of 0.7 mL/min. After injection, the gradient was increased linearly to 28% solvent B over 45 min and then to 100% B over 2 min and held at 100% B for 10 min. Fractions were collected into 2.5 mL of chloroform/methanol (2:1), and 1 mL of PBS was added. The organic phase was recovered, dried under nitrogen, resuspended in 95% ethanol, and stored at −20 °C. Liquid chromatography/mass spectroscopy analysis confirmed the identities of each EET regioisomer (*27*). To prepare the sodium salts of [^{3}H]EETs, an appropriate volume of ethanolic [^{3}H]EET was evaporated under nitrogen and resuspended in 0.1 mM Na_2CO_3 at a concentration of 20−40 μM (specific activity of ∼90 μCi/μmol) and kept on ice. Sodium salts of other fatty acids were prepared in the same manner.

Recombinant FABPs and sEH. Recombinant rat H-FABP was prepared as previously described (*25*) and delipidated by butanol extraction (*28*). Delipidated recombinant rat L-FABP was a generous gift from Dr. Friedhelm Schroeder, Texas A&M University. Recombinant mouse sEH (*29*) was a generous gift of Dr. Bruce Hammock, University of California, Davis. A specific activity of ∼18 μmol min^{-1} mg^{-1} was measured using 1,3-transdiphenylpropene oxide as substrate (*30*).

sEH Activity Measurement. A working stock of 13 nM sEH was prepared in assay buffer (50 mM Tris-Cl, pH 7.5, 150 mM KCl) containing 0.75 μM BSA and kept on ice. [^{3}H]11,12-EET or [^{3}H]14,15-EET (final concentrations of 0.2−5 μM) was added to 155 μL of assay buffer containing 5 nM BSA in glass vials. Reactions were initiated by adding sEH to final concentrations of 0.2 or 0.4 nM and incubated for 1−4 min at 30 °C as specified in the figure legends. The final BSA concentration was 30 nM. No radiolabeled DHET was detected in control reactions in the absence of sEH either with or without FABP. Reaction mixtures that included FABP and fatty acid antagonists or vesicles were incubated for 2 min prior to enzyme addition. Small unilamellar vesicles were prepared from egg phosphatidylcholine (*31*). Reactions were terminated by transfer into 5 mL of chloroform/methanol (2:1), followed by addition of 1 mL of 0.9% saline. Tubes were vortexed and centrifuged for 10 min at 4 °C. The bottom layer was removed and saved, and the top layer was re-extracted with 1 mL of chloroform/methanol/0.9% saline (86:14:1). The bottom phases were combined, dried under nitrogen, and resuspended in chloroform/methanol (2:1) containing 0.4 μg/μL of a neutral lipid standard mixture (18-5C, NuChek Prep, Elysian, MN). The samples were applied to silica gel G thin-layer chromatography plates and developed to 4 cm in chloroform/methanol/acetic acid (60:30:1). The plate was dried and then further developed in hexane/ethyl acetate/acetic acid (70:30:1). TLC plates were analyzed with a radioisotope scanner (Bioscan, Washington, DC) (*30*). Two radioactive peaks were detected and identified as EET and DHET by comigration with standards. Peak areas were determined with Bioscan software, and DHET production was quantified by multiplying the total pmol of reaction substrate by the fractional DHET peak area.

Estimation of Kinetic Parameters and Comparative Modeling. DHET production velocities collected at various EET concentrations were used to estimate K_m and k_{cat} for sEH conversion of EET employing the Michaelis−Menten model and nonlinear least-squares regression using DynaFit (*32*). Average substrate quantities (S_{avg}), calculated from $S_{avg} = S_{ini} - (P/2)$, where S_{ini} = initial pmol of substrate and P = pmol of product, were used for parameter estimation in some samples where 20−60% of the substrate was converted during the reaction.

DHET production velocities were collected at various FABP concentrations and fit to inhibition models by least-squares nonlinear regression using DynaFit. Equilibrium steps were assumed to be in the rapid limit. For this modeling analysis, K_m and k_{cat} were set to values determined on the same day under identical conditions in the absence of FABP. Comparison of the goodness of fit between models was performed with the model discrimination module of DynaFit. The inhibition models employed were

(1) competitive inhibition:

$$\text{sEH} + \text{FABP} \overset{K_i}{\rightleftharpoons} \text{sEH·FABP}$$

$$\text{EET} + \text{sEH} \overset{K_m}{\rightleftharpoons} \text{sEH·EET} \xrightarrow{k_{cat}} \text{sEH} + \text{DHET}$$

(2) substrate depletion:

$$\text{EET} + \text{FABP} \overset{K_d}{\rightleftharpoons} \text{FABP·EET}$$

$$\text{EET} + \text{sEH} \overset{K_m}{\rightleftharpoons} \text{sEH·EET} \xrightarrow{k_{cat}} \text{sEH} + \text{DHET}$$

(3) noncompetitive inhibition:

$$\text{sEH} + \text{FABP} \overset{K_i}{\rightleftharpoons} \text{sEH·FABP}$$

$$\text{sEH·EET} + \text{FABP} \overset{K_i}{\rightleftharpoons} \text{sEH·EET·FABP}$$

$$\text{EET} + \text{sEH} \overset{K_m}{\rightleftharpoons} \text{sEH·EET} \xrightarrow{k_{cat}} \text{sEH} + \text{DHET}$$

Progress Curve Simulation. Progress curves for a model EET pathway were simulated using DynaFit, starting with rapid production of a total of 1 μM EET at an appearance rate of 0.01 s^{-1} starting at time 0. Model sEH catalytic values were set at K_m = 0.45 μM and k_{cat} = 9.2 s^{-1}, as determined in the Results. The kinetics of EET binding to H-FABP were set at k_{on} = 49 μM^{-1} s^{-1} and k_{off} = 8.2 s^{-1}, estimated from

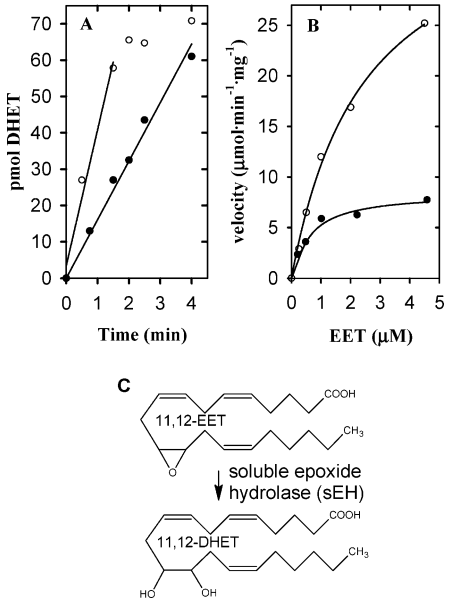

FIGURE 1: Kinetic analysis of EET conversion to DHET by sEH. Racemic [^{3}H]11,12-EET or [^{3}H]14,15-EET in 50 mM Tris-Cl (pH 7.5) and 150 mM KCl containing 30 nM BSA was incubated with 0.4 nM recombinant murine sEH at 30 °C. The lipids were extracted and analyzed by TLC and radiometric scanning. (A) Time courses for DHET production from 90 pmol of 11,12-EET (●) or 14,15-EET (○). (B) Initial velocity plots. The time of incubation was 2 min for 11,12-EET (●) and 1 min for 14,15-EET (○). The lines were generated by nonlinear least-squares fitting to the Michaelis−Menten model. (C) Structures of 11,12-EET and 11,12-DHET.

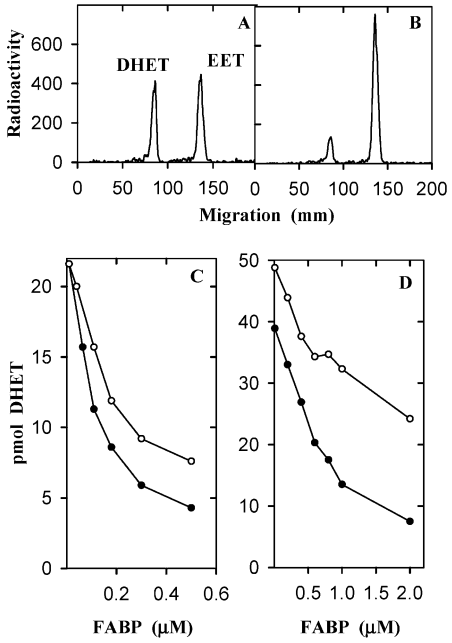

FIGURE 2: Inhibition of EET conversion to DHETs by FABPs. [^{3}H]11,12-EET or [^{3}H]14,15-EET was incubated with FABP for 2 min prior to addition of sEH. Panels A and B are representative radiometric scans of TLC plates. (A) [^{3}H]DHET production in the absence of FABP. (B) [^{3}H]DHET production in the presence of 0.18 μM rat H-FABP. (C) Inhibition of [^{3}H]11,12-EET (0.4 μM) conversion to DHET by rat H-FABP (●) or rat L-FABP (○). (D) Inhibition of [^{3}H]14,15-EET (0.6 μM) conversion to DHET by rat H-FABP (●) or rat L-FABP (○). The incubation time was 1 min.

the k_{on} value for arachidonic acid association with rat H-FABP (*33*) and the K_d for H-FABP binding of 11,12-EET determined experimentally. The concentration of sEH was set at 0.01 μM. An output pathway, competing with sEH for metabolism of EET, was set at a rate of 0.01 s^{-1}.

RESULTS

Determination of K_m and V_{max} of sEH for 11,12-EET. Previous studies of sEH catalysis of epoxy-containing fatty acids utilized an assay buffer that included 100 μg/mL phospholipid vesicles (*20*) or 1.5 μM BSA (*34*) to assist solubilization of fatty acids and to stabilize sEH. We found that inclusion of 30 nM BSA in the reaction buffer was sufficient to stabilize sEH activity and allow kinetic measurement of radiolabeled EET conversion by sEH. Under these conditions, [^{3}H]11,12-DHET production was linear with time for at least 3 min, while the production of [^{3}H]14,15-DHET was linear up to 1 min (Figure 1A). The resultant initial velocities for the conversion of 11,12-EET to 11,12-DHET were well-fit by the Michaelis−Menten model (Figure 1B). The kinetic parameters for 11,12-EET determined from nonlinear regression of the velocity data were $K_m = 0.45 \pm 0.08$ μM and $V_{max} = 9.2 \pm 1.4$ μmol min^{-1} mg^{-1} ($n = 3$). The regioisomer, 14,15-EET, was also efficiently utilized in this assay system ($K_m = 2.5$ μM; $V_{max} = 38$ μmol min^{-1} mg^{-1}).

FABP Inhibition of EET Conversion by sEH. The effects of delipidated rat H-FABP and L-FABP on the conversion of [^{3}H]11,12-EET and [^{3}H]14,15-EET by sEH were examined. DHETs are not expected to compete with EETs for FABP binding under these assay conditions since FABP affinities for EETs are ~20-fold greater than those for DHETs (*25*). Comparison of TLC radiochromatograms of reactions in the absence (Figure 2A) or presence of H-FABP (Figure 2B) shows that H-FABP substantially diminished 11,12-DHET production. Both H-FABP and L-FABP were potent, concentration dependent inhibitors of sEH-mediated 11,12-EET conversion to 11,12-DHET (Figure 2C), affording substantial inhibition at nanomolar concentrations. No inhibition of 11,12-EET conversion was observed with 5 μM soybean trypsin inhibitor, indicating that the inhibition of DHET production did not occur in a nonspecific manner (data not shown). Conversion of the 14,15-EET regioisomer was likewise substantially reduced by both H-FABP and L-FABP (Figure 2D), although higher concentrations of FABP were required as compared to the 11,12-EET regioisomer. This is consistent with the ~4-fold weaker affinity of FABP for 14,15-EET as compared to 11,12-EET (*25*).

Modeling of H-FABP Inhibition. To explore the mechanism of inhibition, rates of EET conversion to DHET were collected at an array of initial H-FABP and EET concentrations (Figure 3). To provide additional mechanistic information, these experiments were conducted at two sEH concentrations. All data were simultaneously fit to models of competitive inhibition (Figure 3A), substrate depletion (Figure 3B), and noncompetitive inhibition (Figure 3C). The substrate depletion model was more predictive than either competitive inhibition or noncompetitive inhibition ($P < 0.001$), and only the substrate depletion model was able to replicate the upward-concave shape observed at higher H-FABP concentrations (Figure 3B). The best fit substrate depletion model yielded a K_d for H-FABP binding of 11,12-EET of 0.17 ± 0.01 μM, similar to the K_d' determined by the fluorescence-competitor displacement assay of 0.37 μM (*25*).

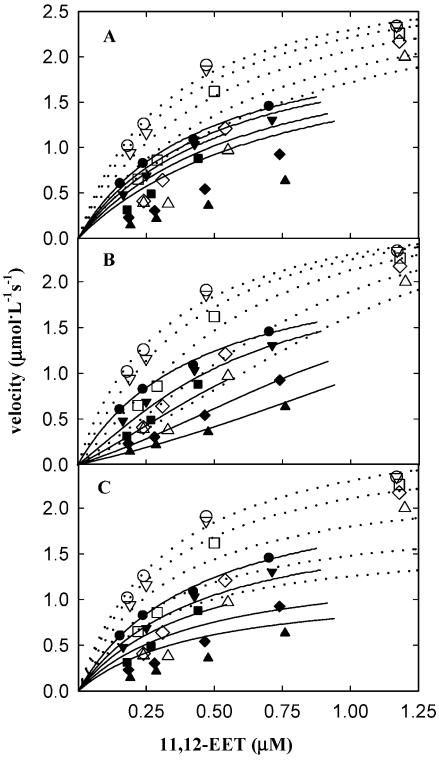

FIGURE 3: Modeling of H-FABP inhibition of sEH. Various concentrations of [^{3}H]11,12-EET and H-FABP were incubated for 2 min prior to addition of sEH. Data from two experiments are shown. H-FABP concentrations in the open symbol data set were 0 (○), 0.2 (▽), 0.4 (□), 0.7 (◇), and 1.1 μM (△). The final concentration of sEH was 0.4 nM. H-FABP concentrations in the filled symbol data set were 0 (●), 0.1 (▼), 0.3 (■), 0.6 (♦), and 0.9 μM (▲). The final concentration of sEH was 0.2 nM. The data from both experiments were fit simultaneously by nonlinear regression to models for competitive inhibition (A), substrate depletion (B), and noncompetitive inhibition (C). Dotted lines were generated from the open symbol data set and the solid lines from the closed symbol data set. Analysis of the substrate depletion model yielded a K_d of 0.17 ± 0.01 μM.

Antagonism of H-FABP Inhibition by FABP Ligands. The effects of several FABP ligands on FABP inhibition of 11,12-EET conversion were examined. In these experiments, H-FABP was present at a concentration that inhibited DHET production by ~65% (Figure 4A). We found that arachidonic acid, a high affinity ligand for H-FABP with K_d = 50 nM (*35*), restored product formation in reactions containing H-FABP (Figure 4B). The effect was dose dependent, such that 1.5 μM arachidonic acid, a concentration expected to nearly completely displace EET from H-FABP, was able to restore the full rate observed in the absence of FABP. This is consistent with the substrate depletion model, where a FABP ligand would competitively displace FABP-bound EET, thus relieving inhibition. The addition of arachidonic acid in the absence of FABP did not alter the amount of DHET formed (data not shown), indicating that arachidonic acid alone did not alter the kinetics of EET conversion by sEH.

The effects of three other FABP ligands (oleic acid, linoleic acid, and a cytochrome P450 ω-hydroxylase product, 20-hydroxyeicosatetraenoic acid (20-HETE)) on FABP inhibition were compared to that of arachidonic acid (Figure 5). Oleic acid, and to a lesser extent, linoleic acid, effectively antagonized FABP inhibition of 11,12-EET conversion to

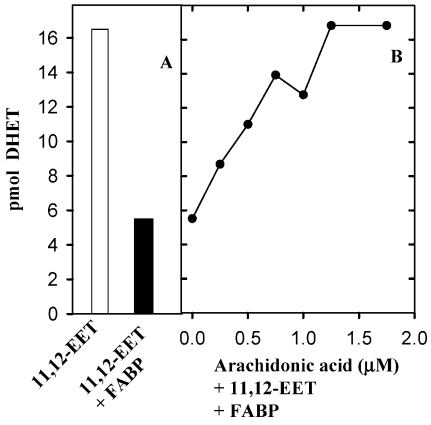

FIGURE 4: Antagonism of H-FABP inhibition by arachidonic acid. Various concentrations of arachidonic acid were incubated with 0.4 μM [^{3}H]11,12-EET and 0.6 μM H-FABP for 2 min prior to addition of sEH. (A) DHET production in the absence (open bar) and presence of H-FABP (filled bar). (B) DHET production in the presence of arachidonic acid and 0.6 μM H-FABP. This experiment was repeated once, and similar results were obtained.

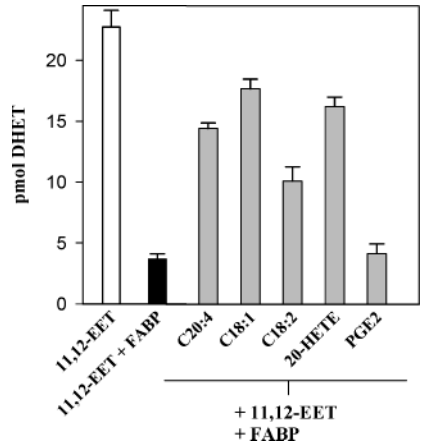

FIGURE 5: Antagonism of H-FABP inhibition by H-FABP ligands. All reactions contained 0.4 μM [^{3}H]11,12-EET and 0.5 μM H-FABP except the leftmost bar, which indicates the amount of DHET formed in the absence of H-FABP. Arachidonic acid (C20:4), oleic acid (C18:1), linoleic acid (C18:2), 20-hydroxyeicosatetraenoic acid (20-HETE), or prostaglandin E_2 (PGE_2) were added at a final concentration of 1.5 μM. Values plotted are the mean ± standard error of triplicate determinations. This experiment was repeated once, and similar results were obtained.

DHET. Like arachidonic acid, these fatty acids are bound tightly by FABPs (*23*). Our previous studies found that H-FABP binds 20-HETE with an affinity similar to 11,12-EET (K_d of 0.4 μM, ref *25*). Figure 5 shows that 20-HETE relieved the inhibition produced by FABP. In contrast, PGE_2 was ineffective in restoring DHET production, consistent with the weak affinity of H-FABP for PGE_2 as determined by a fluorescent displacement binding assay (data not shown). The addition of these fatty acids in the absence of FABP had no effect on product formation by sEH (data not shown).

DISCUSSION

On the basis of our previous finding that FABPs bind EETs, we proposed that FABPs may modulate intracellular EET metabolism and signaling (*25*). One of the major metabolic pathways of EET is the conversion to DHET by sEH (*36*). In the present study, the effects of FABP on the conversion of EET to DHET by sEH were examined. The

major findings are that both H-FABP and L-FABP inhibit the conversion of 11,12-EET and 14,15-EET by sEH. H-FABP inhibition was consistent with a substrate depletion model where FABP:EET complex formation limits the availability of EET to sEH.

Previous kinetic studies of sEH conversion of epoxy fatty acids included either BSA or phospholipid vesicles in the incubation medium to facilitate solubilization of the fatty acids and stabilize sEH activity (*20*, *34*). We utilized an assay buffer containing a concentration of BSA (30 nM) that was sufficient to stabilize sEH activity. Under these conditions, the Michaelis−Menten parameters for sEH conversion of racemic (50:50) 11,12-EET were $K_m = 0.45 \pm 0.08$ μM and $V_{max} = 9.2 \pm 1.4$ μmol min^{-1} mg^{-1}. These values do not appear to be consistent with those of Zeldin et al. (*20*), who determined separate kinetic constants for each 11,12-EET enantiomer: 11(*R*),12(*S*)-EET, $K_m = 3$ μM, $V_{max} = 0.8$ μmol min^{-1} mg^{-1} and 11(*S*),12(*R*)-EET, $K_m = 4$ μM, $V_{max} = 3$ μmol min^{-1} mg^{-1}. The discrepancy might be due to differences in recombinant versus native enzyme preparations or the presence of phosphatidylcholine vesicles (100 μg/mL) in the assay buffer of Zeldin et al. We found that phosphatidylcholine vesicles inhibited 11,12-EET conversion by sEH. Under assay conditions identical to those used to examine FABP inhibition of sEH, egg phosphatidylcholine vesicles inhibited 11,12-EET conversion in a concentration dependent manner, with ~15% reduction of DHET production with 3 μg/mL vesicles and ~60% reduction with 9 μg/mL vesicles (data not shown). Thus, the higher K_m values of Zeldin et al. may be explained by a rightward shift in the velocity curve due to the inaccessibility of vesicle-associated substrate. Our kinetic analysis yielded a catalytic efficiency (k_{cat}/K_m) of 21 μM^{-1} s^{-1} for racemic 11,12-EET, which is 70- and 26-fold higher than the 0.3 and 0.8 μM^{-1} s^{-1} values obtained by Zeldin et al. for 11(*R*),12(*S*)-EET and 11(*S*),12(*R*)-EET, respectively. This suggests that sEH may utilize 11,12-EET more efficiently than previously thought.

An implication of our findings is that FABP may buffer fluctuations in EET concentration, serving as a dynamic intracellular EET reservoir as has been shown for retinoids and retinoid binding proteins and the acyl-CoA binding protein (*37*). Such FABP buffering activity may be especially important during agonist-stimulated phospholipase activation. Phospholipase A_2 stimulation releases large amounts of fatty acids that rapidly accumulate in cytosol and subsequently are released from the cell (*38*). For example, in cultured endothelial cells, [^{3}H]14,15-EET was incorporated into phospholipids and subsequently released into the medium upon stimulation by a calcium ionophore, a nonspecific activator of phospholipases (*17*). In platelets, activation of phospholipases by thrombin resulted in the release of 5−7 fmol of endogenous EET per 10^6 cells, indicating that unesterified EET may have accumulated intracellularly to a concentration of ~1 μM (*39*).

To illustrate the effect of FABP on a theoretical burst release of esterified EET from phospholipids, simulations were performed using the pathway outlined in Figure 6A. The pathway begins with phospholipase A_2 releasing EET from EET-containing phospholipids. In this model, the deacylated EET has three possible fates: conversion to DHET by sEH, binding to FABP, or utilization by alternate pathways/targets, which are labeled as output. Figure 6B shows the total concentration of EET with time for the three conditions tested, no FABP, 1 μM FABP, and 10 μM FABP. Although the total input of EET is the same for each simulation condition, EET buildup is greatly enhanced in both magnitude and duration in the presence of FABP. This is because FABP binding reduces EET flux to the output pathway and conversion to DHET. Figure 6C shows the rate of DHET production. In the absence of FABP, a spike of DHET production occurs. In contrast, the presence of FABP dampens the spike of DHET and prolongs its production. This simulation illustrates that FABP may prolong EET intracellular accumulation by serving as a reversible reservoir for EET.

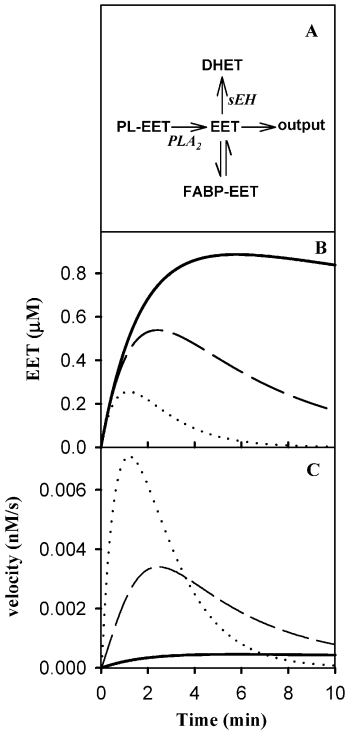

FIGURE 6: Simulation of FABP modulation of EET metabolic pathways. (A) Diagram of EET metabolic pathways analyzed by kinetic simulation. PL-EET represents the storage form of EET (esterified to phospholipids). In this model, phospholipase A_2 (PLA_2) activity releases EET, which is then subject to three fates: reversible binding by FABP, conversion to DHET by sEH, or utilization by other pathways (output). (B) Simulation of total EET concentration with time after a burst input of 0.01 s^{-1} of EET as described in Experimental Procedures. The simulation was run under three conditions: no FABP (dotted line), 1 μM FABP (dashed line), and 10 μM FABP (solid line). (C) Simulated rate of DHET production in the absence of FABP (dotted line), 1 μM FABP (dashed line), and 10 μM FABP (solid line).

The FABP modulation of EET metabolism might have significant functional consequences in the regulation of blood pressure. DHET production is markedly elevated in renal cortical S9 fractions from spontaneously hypertensive rats, and systemic administration of a sEH inhibitor reduced blood pressure in these rats (*21*). Furthermore, disruption of the sEH gene reduced blood pressure in male mice (*22*). These findings imply that maintenance of the proper levels of EETs and DHETs is crucial to the governance of vascular tone, and we suggest FABP binding of EETs in vascular cells may be an important component of blood pressure regulation. Further support for this hypothesis will require characterization of FABP types and sEH activity in resistance vessels.

In addition, transfected cells that overexpress FABP could be utilized to assess the effect of various levels of FABP on EET metabolism.

H-FABP inhibition of EET conversion to DHET was antagonized by fatty acids, consistent with a substrate depletion model where FABP ligands such as unesterified fatty acids would limit the ability of FABP to sequester EET from sEH. This could have an important impact on EET metabolism in vivo when fatty acid levels are elevated, leading to an increase in sEH-mediated conversion to DHET. Such an effect might contribute to the impaired vasodilation in conduit vasculature and impaired fibrinolysis that occur following a high fat meal when fatty acids are elevated (*40*, *41*).

In conclusion, our findings indicate that FABPs limit EET availability to sEH. The equilibration of EET with FABP binding sites may create an intracellular EET reservoir that meters out EET among its metabolic pathways. Thus, vascular cell FABP may be an important component of the EET-based regulation of vascular tone. Furthermore, alterations of FABP ligation by fluctuations in intracellular unesterified fatty acid levels could have important consequences for cellular metabolism of EET.

ACKNOWLEDGMENT

We thank Bruce Hammock and Christophe Morisseau (University of California, Davis) for supplying sEH, and Friedhelm Schroeder (Texas A&M University) for supplying L-FABP. We also thank Bruce Hammock, Christophe Morisseau, and James Gray (University of Iowa) for critical review of the manuscript.

REFERENCES

1. Campbell, W. B., and Harder, D. R. (1999) *Circ. Res. 84*, 484−8.
2. Capdevila, J. H., Falck, J. R., and Harris, R. C. (2000) *J. Lipid Res. 41*, 163−81.
3. Roman, R. J. (2002) *Physiol. Rev. 82*, 131−85.
4. Kroetz, D. L., and Zeldin, D. C. (2002) *Curr. Opin. Lipidol. 13*, 273−83.
5. Hu, S., and Kim, H. S. (1993) *Eur. J. Pharmacol. 230*, 215−21.
6. Campbell, W. B., Gebremedhin, D., Pratt, P. F., and Harder, D. R. (1996) *Circ. Res. 78*, 415−23.
7. Fisslthaler, B., Popp, R., Kiss, L., Potente, M., Harder, D. R., Fleming, I., and Busse, R. (1999) *Nature 401*, 493−7.
8. Node, K., Ruan, X. L., Dai, J., Yang, S. X., Graham, L., Zeldin, D. C., and Liao, J. K. (2001) *J. Biol. Chem. 276*, 15983−9.
9. Node, K., Huo, Y., Ruan, X., Yang, B., Spiecker, M., Ley, K., Zeldin, D. C., and Liao, J. K. (1999) *Science 285*, 1276−9.
10. Chen, J. K., Falck, J. R., Reddy, K. M., Capdevila, J., and Harris, R. C. (1998) *J. Biol. Chem. 273*, 29254−61.
11. Chen, J. K., Capdevila, J., and Harris, R. C. (2000) *J. Biol. Chem. 275*, 13789−92.
12. Cowart, L. A., Wei, S., Hsu, M. H., Johnson, E. F., Krishna, M. U., Falck, J. R., and Capdevila, J. H. (2002) *J. Biol. Chem. 277*, 35105−12.
13. Zhang, Y., Oltman, C. L., Lu, T., Lee, H. C., Dellsperger, K. C., and VanRollins, M. (2001) *Am. J. Physiol. 280*, H2430−40.
14. Fang, X., Weintraub, N. L., Oltman, C. L., Stoll, L. L., Kaduce, T. L., Harmon, S., Dellsperger, K. C., Morisseau, C., Hammock, B. D., and Spector, A. A. (2002) *Am. J. Physiol. 283*, H2306−14.
15. Bernstrom, K., Kayganich, K., Murphy, R. C., and Fitzpatrick, F. A. (1992) *J. Biol. Chem. 267*, 3686−90.
16. VanRollins, M., Kaduce, T. L., Fang, X., Knapp, H. R., and Spector, A. A. (1996) *J. Biol. Chem. 271*, 14001−9.
17. Weintraub, N. L., Fang, X., Kaduce, T. L., VanRollins, M., Chatterjee, P., and Spector, A. A. (1997) *Circ. Res. 81*, 258−67.
18. Fang, X., Weintraub, N. L., and Spector, A. A. (2003) *Prostaglandins & Other Lipid Mediators 71*, 33−42.
19. Zeldin, D. C., Kobayashi, J., Falck, J. R., Winder, B. S., Hammock, B. D., Snapper, J. R., and Capdevila, J. H. (1993) *J. Biol. Chem. 268*, 6402−7.
20. Zeldin, D. C., Wei, S., Falck, J. R., Hammock, B. D., Snapper, J. R., and Capdevila, J. H. (1995) *Arch. Biochem. Biophys. 316*, 443−51.
21. Yu, Z., Xu, F., Huse, L. M., Morisseau, C., Draper, A. J., Newman, J. W., Parker, C., Graham, L., Engler, M. M., Hammock, B. D., Zeldin, D. C., and Kroetz, D. L. (2000) *Circ. Res. 87*, 992−8.
22. Sinal, C. J., Miyata, M., Tohkin, M., Nagata, K., Bend, J. R., and Gonzalez, F. J. (2000) *J. Biol. Chem. 275*, 40504−10.
23. Richieri, G. V., Ogata, R. T., Zimmerman, A. W., Veerkamp, J. H., and Kleinfeld, A. M. (2000) *Biochemistry. 39*, 7197−204.
24. Luxon, B. A., and Milliano, M. T. (1999) *Am. J. Physiol. 277*, G361−6.
25. Widstrom, R. L., Norris, A. W., and Spector, A. A. (2001) *Biochemistry 40*, 1070−6.
26. Antohe, F., Popov, D., Radulescu, L., Simionescu, N., Borchers, T., Spener, F., and Simionescu, M. (1998) *Eur. J. Cell Biol. 76*, 102−9.
27. Fang, X., Kaduce, T. L., Weintraub, N. L., Harmon, S., Teesch, L. M., Morisseau, C., Thompson, D. A., Hammock, B. D., and Spector, A. A. (2001) *J. Biol. Chem. 276*, 14867−74.
28. Cham, B. E., and Knowles, B. R. (1976) *J. Lipid Res. 17*, 176−81.
29. Grant, D. F., Storms, D. H., and Hammock, B. D. (1993) *J. Biol. Chem. 268*, 17628−33.
30. Borhan, B., Mebrahtu, T., Nazarian, S., Kurth, M. J., and Hammock, B. D. (1995) *Anal. Biochem. 231*, 188−200.
31. Kamp, F., Hamilton, J. A., and Westerhoff, H. V. (1993) *Biochemistry 32*, 11074−86.
32. Kuzmic, P. (1996) *Anal. Biochem. 237*, 260−73.
33. Richieri, G. V., Ogata, R. T., and Kleinfeld, A. M. (1996) *J. Biol. Chem. 271*, 11291−300.
34. Moghaddam, M., Motoba, K., Borhan, B., Pinot, F., and Hammock, B. D. (1996) *Biochim. Biophys. Acta 1290*, 327−39.
35. Richieri, G. V., Ogata, R. T., and Kleinfeld, A. M. (1994) *J. Biol. Chem. 269*, 23918−30.
36. Zeldin, D. C. (2001) *J. Biol. Chem. 276*, 36059−62.
37. Noy, N. (2000) *Biochem. J. 348*, 481−95.
38. Chilton, F. H., Fonteh, A. N., Surette, M. E., Triggiani, M., and Winkler, J. D. (1996) *Biochim. Biophys. Acta 1299*, 1−15.
39. Zhu, Y., Schieber, E. B., McGiff, J. C., and Balazy, M. (1995) *Hypertension 25*, 854−9.
40. Vogel, R. A., Corretti, M. C., and Plotnick, G. D. (1997) *Am. J. Cardiol. 79*, 350−4.
41. Anderson, R. A., Jones, C. J., and Goodfellow, J. (2001) *Atherosclerosis 159*, 9−15.

BI034971D